

Structured modelling from data and optimal control of the cooling system of a large business center

E. Terzi^a, L. Fagiano^a, M. Farina^a, R. Scattolini^a

^a*Dipartimento di Elettronica, Informazione e Bioingegneria, Politecnico di Milano, Milan 20133, Italy*

(email: {enrico.terzi,lorenzo.fagiano,marcello.farina,riccardo.scattolini}@polimi.it)

Abstract

The optimal cooling operation of a large business center, with five buildings totalling about 70,000 m² of interiors, is considered. This problem is relevant due to the high operational costs and energy demand of the cooling system. The latter features four chillers currently managed with heuristic rules. The aim of this study is to redesign the control system to minimize the energy consumption while still meeting the cooling demand. The main challenges are the impossibility to derive a model of the system based on physics, due to its high complexity and lack of information on each subsystem, and the on-off behaviour and hysteretic operational constraints of the chillers. To solve this problem, a structured black-box dynamical model of the system is derived using machine learning techniques, exploiting a dataset of more than 500 days of operation. The employed quantities are easily measurable and include the flow rate and temperature of the cooling water, electric power consumption, and external temperature and humidity. Then, the derived model has been used to optimally tune the feedback control strategy via nonlinear programming, by minimizing the predicted energy consumption while satisfying the cooling demand. Simulation results with a validation dataset indicate that the proposed approach achieves an energy saving of 30% with respect to the controller currently adopted, while keeping the temperature in the desired range. The proposed modelling approach, based on data, results in a high applicability to plants with different layouts and components, whenever measurements of the relevant quantities are available.

Keywords: Cooling station, control for energy saving, identification, modelling, optimization, HVAC systems.

1. Introduction

The topic of energy saving in buildings by optimization of their cooling plants is receiving a growing interest, see for example [13], [18], [3], [29], [26], [19], [22]. This trend is motivated by the large share, over 38% according to [2], of the overall energy consumption attributable to buildings; within that, about 50% pertains to Heating Ventilation and Air Conditioning (HVAC) systems,

see [21]. Notably, this percentage grows up to 76 % in European countries, see [16], making this issue of pivotal importance. In this kind of plants, it is typical to use simple rule-based logics [20] that allow to run the system in a satisfactory but non efficient way, so that there is room for the development of smarter solutions. The attention to this topic also results in private and public incentives to enhance energy-efficient solutions, for both environment preservation and economic convenience. From public institutions, many certificates for sustainability of buildings have been devised, such as the Leadership in Energy and Environmental Design (LEED) given by the U.S. Green Building Council, see [8], together with guidelines to assess energy performances of buildings, see [14].

In the literature, modeling and control of HVAC systems have been discussed by several authors. Among the several contributions related to the modeling approaches, [13] relies on physical equations, intrinsically needing a lot of prior information, and takes advantage of the possibility of performing experimental tests on the plant, while [18] develops a predictive control strategy based on an electric equivalent of the network, whose layout is fully known. In [26] the model of the system is developed only for the cooling station, without including the users; indeed, the modular approach proposed therein is based on nonlinear physical equations of each component, similarly to [24]. A completely different approach is proposed in [29], where the whole plant is described by means of a comprehensive neural network, that turns out to be effective, but does not allow to have physical insights of the phenomena, and makes it difficult to exploit the, possibly little, prior information available. Neural models trained from data are also exploited in [30], where the focus is on the cooling load prediction, without comprising the whole cooling station. Also, a collection and comparison of different black-box modeling approaches for HVAC systems is reported in [1], where a relatively small residential system is considered.

Regarding the control strategy, many authors propose the adoption of advanced control techniques, see for example [23], [4], [12], though these schemes often entail several issues for their practical implementation [7]. A number of approaches has been proposed to simplify their design and deployment, among these it is possible to recall the recent contributions [9] and [25] relying on machine learning tools. However, the deployment and installation of a novel controller still remains a crucial issue, even more when it needs measurements from several devices placed over the typically large and distributed HVAC station.

In this article we first derive a complete dynamic model of the cooling station of a large commercial site located in Milan, northern Italy, then we use this model for control design, ending with a ready-to-use solution. Preliminary results on the identification stage are reported in [27], and here they are extended and completed with the control optimization. The commercial center is composed of five buildings with fifteen floors each, see Figure 1 for an aerial view of the site. The buildings are almost totally devoted to offices and commercial spaces, but there are also two server rooms, a canteen, an auditorium and other facilities. In working days (Monday-Friday), it is estimated that about 7000

people occupy this center, about 2000 people are present on Saturdays, while on Sunday the main thermal load is due to the servers, except for extra events, such as conferences and meetings. A unique cooling station is in charge of providing cold water for air-conditioning in spring and summer to the offices, and to disperse the heat produced by the servers and data centers over the whole year, that indeed constitute a non-negligible permanent load.

Due to the complexity of the problem, to the lack of fundamental information on the size and behavior of many devices, and to the uncertain knowledge of the users' demand and operating conditions, a purely physical modeling approach would be hardly feasible. On the other hand, with a totally black-box approach, the fundamental a-priori information on the plant layout would be lost and the achieved results could not be given the physical insight required to interpret and rely on the identified models. These reasons have suggested to adopt a *structured black-box approach*, based on the decomposition of the large-scale plant into smaller subsystems, connected through known quantities. In the modeling of the subsystems, all the available physical information has been used to select the structure of the linear and nonlinear dynamic models, which have been identified starting from the very large set of data available, related to more than 500 days of operation, with more than 400 recorded variables. The obtained models of the subsystems have been tested singularly and then linked together. The overall model of the plant so obtained has proven to capture the main system's dynamics without being too complex, and for this reason it has been used in the control design phase.

The commercial center is already controlled with a relay-based logic acting on the switch on/off of the chillers. In order to obtain immediately applicable results, not requiring any structural change of the existing control system, it has been decided to optimize the parameters of the existing logic, i.e. the thresholds on the temperatures governing the switch on/off of the chillers and the idle time between successive switches, with the main goal to minimize the energy consumption. Considering a period of one week, an optimization problem has been formulated by minimizing a cost function penalizing the energy consumption and the users' discomfort, and by including physical constraints on the plant variables. By relying on the identified model, the optimal solution has been computed in terms of thresholds and idle time variations with respect to the nominal (currently applied) values. The results achieved, tested in simulation with the model over one week-long period, show that roughly 30% of energy savings can be obtained with respect to the existing solution, thanks to control optimization.

The paper is organized as follows. In Section 2 the overall cooling station is presented. In Section 3 the model identification approach and the adopted criteria for model structure selection are described. Section 4 concerns the problems and the results achieved in the identification of the main subsystems, namely the chillers, the pipes and the users. In Section 5 the overall model, composed of the previously identified subsystems, is built and its performance is compared with the measured data in closed-loop validation. Lastly, Section 6 describes the current control logic, the design of the optimized one and compares



Figure 1: Business/Commercial area considered in this paper

their performance in the simulated environment. Conclusions and directions for future work are discussed in Section 7.

A list of the variables and parameters pertaining to the system follows, where $t \in \mathbb{Z}$ denotes the discrete time variable:

Parameters			
Quantity	Description	Value	Unit
T_s	Sampling time	60	s
w_{ch}	Nominal cooled water flow rate through each chiller	355	m^3/h
w_{abs}	Nominal cooled water flow rate through the absorber	310	m^3/h
T_r^{sp}	Setpoint for the cooled water temperature from the chiller	8	$^{\circ}C$
T_t^{abs}	Threshold temperature difference used to derive the status of the absorber	0.5	$^{\circ}C$
k	Overall heat transfer coefficient for pipes	50	$\frac{W}{m^2K}$
c_w	specific heat of water	4.186	$\frac{kJ}{kgK}$
ρ_w	density of water	1000	$\frac{kg}{m^3}$
Control logic parameters			
Quantity	Description	Value	Unit
ΔT_{temp}	dwelt-time for temperature conditions that enable switching on/off chillers	300	s
D_t	idle-time after a switch in the control logic	600	s
Variables			
Quantity	Description	Value	Unit
$T_i(t)$	Water temperature at the delivery manifold	$\in \mathbb{R}$	$^{\circ}C$
$T_r^i(t)$	i^{th} chiller outlet water temperature	$\in \mathbb{R}$	$^{\circ}C$
$T_{in}^i(t)$	i^{th} chiller inlet water temperature	$\in \mathbb{R}$	$^{\circ}C$
$T_{ext}(t)$	External temperature	$\in \mathbb{R}$	$^{\circ}C$

$H_{ext}(t)$	External relative humidity	$\in [5, 95]$	/
$w_{off}(t)$	Total water flow rate through the chillers in off state	$\in \mathbb{R}$	m^3/h
$w_{on}(t)$	Total water flow rate through the machines (chiller+absorber) in on state	$\in \mathbb{R}$	m^3/h
$T_r^{on}(t)$	Weighted average temperature of the on machines	$\in \mathbb{R}$	$^{\circ}C$
$n_{on}(t)$	Number of active machines	$\in \{0, 1, 2, 3, 4, 5\}$	/
$s_i(t)$	State of the i^{th} chiller	$\in \{0, 1\}$	/
$P_{ch}^i(t)$	Power absorbed by chiller i	$\in \mathbb{R}$	kW
$v^i(t)$	Normalized rotational speed of fans on evaporative tower of i^{th} chiller	$\in [0, 100]$	%
$T_r^{abs}(t)$	Cooled water outlet temperature from the absorber	$\in \mathbb{R}$	$^{\circ}C$
$T_{in}^{abs}(t)$	Cooled water inlet temperature in the absorber	$\in \mathbb{R}$	$^{\circ}C$
$s_{abs}(t)$	State of the absorber	$\in \{0, 1\}$	/
$w_{bp}(t)$	Bypass flow rate	$\in \mathbb{R}$	m^3/h
$w_t(t)$	Total flow in the primary loop	$\in \mathbb{R}$	m^3/h
$w_{hot}(t)$	Flow in the secondary loop	$\in \mathbb{R}$	m^3/h
$T_{hot}(t)$	Weighted average of the temperatures at the return collectors	$\in \mathbb{R}$	$^{\circ}C$
$Q_u(t)$	Thermal power provided by the users	$\in \mathbb{R}$	kW
$Q_u^j(t)$	Thermal power provided by the j^{th} end-user	$\in \mathbb{R}$	kW
$T_{in}^j(t)$	Inlet temperature measure on end-user j	$\in \mathbb{R}$	$^{\circ}C$
$T_{out}^j(t)$	Outlet temperature measure on end-user j	$\in \mathbb{R}$	$^{\circ}C$
$w_u^j(t)$	Flow rate through user j	$\in \mathbb{R}$	m^3/h
$Q_{pipes}(t)$	Thermal power exchanged through the pipes	$\in \mathbb{R}$	kW
$Q_{refr}(t)$	Cooling power provided by the cooling machines	$\in \mathbb{R}$	kW

2. Plant description

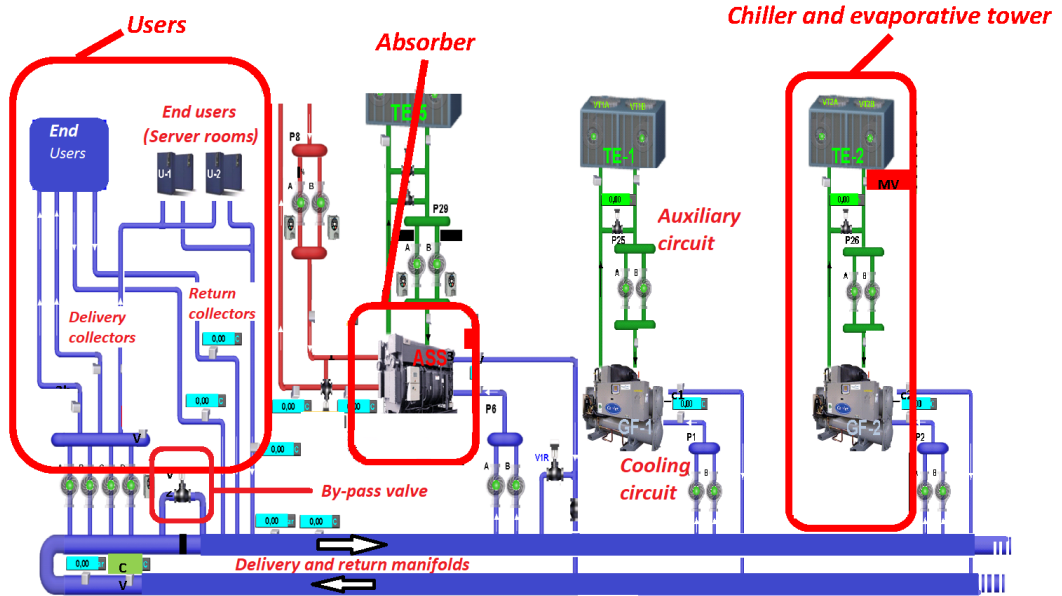


Figure 2: Schematic of the system under analysis

The schematic of the cooling system is shown in Figure 2, while a conceptual representation is reported in Figure 3. The main components are:

- Primary and secondary loops.** In the system, two loops can be distinguished. The *primary loop* comprises the delivery manifold, the by-pass valve, and the return manifold. The loop is closed across the chillers and the absorber, and two measures of the water temperature are available: $T_i(t)$ on the delivery manifold and $T_o(t)$ on the return manifold (see Figure 3). The bypass valve directly links the delivery and return manifolds, it is usually 100% open and it is needed to balance the flowrates of the loops, in order to avoid overpressure and possible damage to the pumps. Its pressure drop, its flowrate $w_{bp}(t)$, and its characteristic curve were not available for our study. Based on the experience of plant operators, a rough estimate of the total flowrate $w_t(t)$ circulating in the primary loop is $900 \text{ m}^3/\text{h}$ during summer days.

The *secondary loop* directs water from the primary loop to the users and drives it back after use. No parameters regarding length, sections, materials, geometry, deployment, and piping network configuration were available. The water splits in three collectors, feeding different groups of end-users, both on the forward line and on the return line, and the water temperature is measured on each of the six collectors. Four modulating

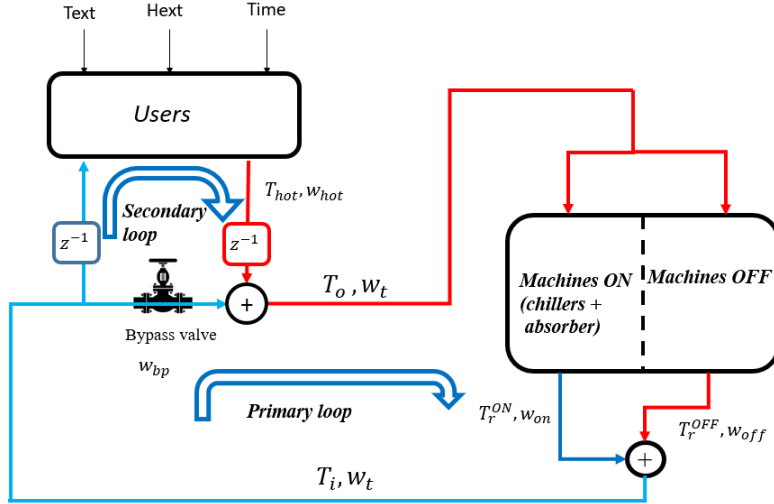


Figure 3: Topology of the system

pumps move water from the primary loop, they are controlled to maintain a delivery pressure; no measures are available. The pipes of the secondary-loop, from the cooling station to the end-users, can be tens of meters long, so that the physical transport delays are not negligible. In addition, the effects of solar radiation and thermal exchange with the environment cannot be neglected.

- Four **chiller units** (in Figure 2 only two are shown for clarity and space limitations). The chillers are thermal machines that cool water from the return manifold and send it to the delivery manifold; the subtracted heat is dispersed in the external environment by means of an evaporative tower. The chillers are connected in parallel and are activated by the control logic, being the only controllable components of the whole plant. They are linked to two circuits: the *condenser, or auxiliary circuit* (in green in Figure 2) that circulates water to the evaporative towers, and the *cooling circuit* (in blue in the figure). In the cooling circuit, each chiller is fed by pumps drawing hot water from the users through a return manifold. These pumps operate only in discrete on/off states; when switched on, they provide a water flowrate that is not measured, so we assumed it constant and equal to its nominal value w_{ch} for each chiller. This on/off behavior represents a bottleneck for an efficient operation, since the efficiency of the HVAC systems critically depends on their load, see [5], which should be varied in order to optimize their power consumption. A scheme of the chiller/tower group is shown in Figure 4, where in dashed red we mark the pipes with higher water temperature, and in solid blue the ones with

lower temperature. The evaporative tower disperses heat by means of controlled modulating fans. No details are available about the pumping units, the pipe lengths, the controller of the fans, and the adopted setpoint. Each chiller embeds a compressor, absorbing energy, that stabilizes the outlet temperature $T_r^i(t)$ to the required set-point T_r^{sp} when a feasible load is demanded. Based on the available dataset, this condition is always satisfied, and we assume it will hold from now on.

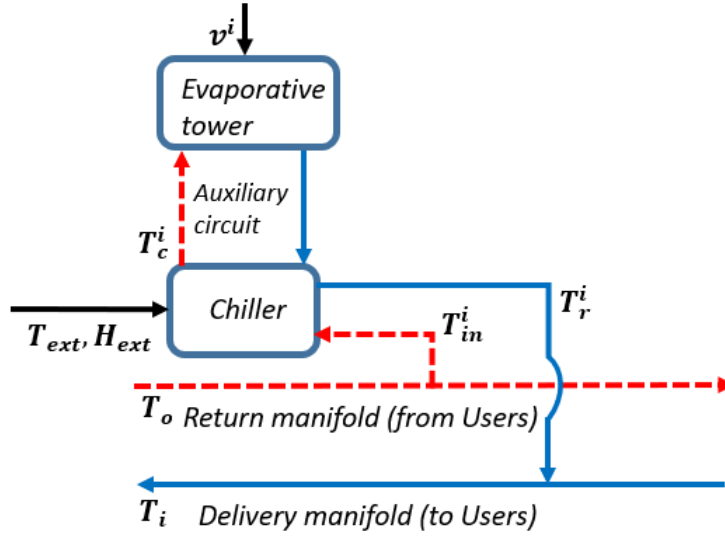


Figure 4: Chiller and evaporative tower

- An **absorber**. The absorber is a thermal machine that exploits the waste heat provided by external systems, such as boilers or heat generators, to refrigerate water; for this reason it is used whenever possible to increase the efficiency of the overall cooling station. It is also equipped with an evaporative tower and it is used in parallel configuration with the chillers. Inside the absorber, complex reactions take place, see [6], its physical modeling is highly complex, and infeasible in our case due to the lack of information about its parameters, and its on/off status during the considered time period. The absorber represents the main unknown disturbance of the overall system, since, when turned on, the pumps circulate a nominal cooled flowrate w_{abs} , of the same order of magnitude as w_{ch} . As for the cooled outlet temperature $T_r^{abs}(t)$, it often does not settle to any setpoint, and varies depending on the thermal power provided to the absorber.
- **Users**. The users comprise offices, commercial spaces, meeting rooms etc., distributed over the five buildings and the fifteen floors. They receive water from the three collectors after the pumping unit. The water returns

at a higher temperature, which depends on the users' thermal load. In total the users are divided into eight groups ("end-users" in Figure 2), with inlet and outlet temperature measures, denoted $T_{in}^j(t)$ and $T_{out}^j(t)$, $j = 1, \dots, 8$, respectively.

3. Preliminary data analysis for model identification

As a first step, outliers and infeasible records have been removed from the available data set. Then, average values have been computed when multiple sensors measure the same physical quantity, to this regard note that no prior information is available on the characteristics of the sensors.

By inspection of the dataset, the (unknown) set-point T_r^{sp} used for control of the water temperature in the delivery manifold has been estimated equal to 8°C .

A non marginal water flowrate, $w_{off}(t)$, passes through the chillers also in off conditions, but no measures are available. A coarse estimate, based on some spot measurements, is 30% of w_{ch} per chiller. Note that, since the water flowrate through the overall closed-loop circuit is related, through an unknown relation, to the loads and to the request by the users, w_{off} is fundamental to guarantee the proper mass balance along the circuit.

Also the state of the chillers is unknown, so that we reconstructed it *a-posteriori* by checking their power consumption $P_{ch}^i(t)$, $i = 1, 2, 3, 4$. More precisely, we defined a binary variable $s_i(t)$ indicating the state of the chiller, such that:

$$s_i(t) = \begin{cases} 1 & P_{ch}^i(t) > 0 \\ 0 & P_{ch}^i(t) = 0 \end{cases} \quad i = 1, 2, 3, 4 \quad (1)$$

Contrarily to the chillers, the absorber on/off status can not be estimated from power consumption, since the machine is not connected to any electrical power source, nor it is recorded. For this reason, we estimated it based on the inlet-outlet temperature difference in the *cooling circuit*, and with a threshold T_t^{abs} to account for measurement noise and avoid high frequency (fictitious) switching. More precisely, we defined a binary variable $s_{abs}(t)$ such that:

$$s_{abs}(t) = \begin{cases} 1 & T_r^{abs}(t) - T_{in}^{abs}(t) < T_t^{abs} \\ 0 & otherwise \end{cases} \quad (2)$$

The water flowrate $w_u^j(t)$, $j = 1, \dots, 8$, in each of the eight pipes to the end-users is measured, so that the total water flowrate circulating in the secondary loop can be computed as:

$$w_{hot}(t) = \sum_{j=1}^8 w_u^j(t) \quad (3)$$

The variable $w_{hot}(t)$, along a week, is reported in Figure 5, its variations are in the range $700 - 850 \text{ m}^3/\text{h}$ save for significant drops, occurring typically at night.

Three sets of temperature measurements are available concerning the users:

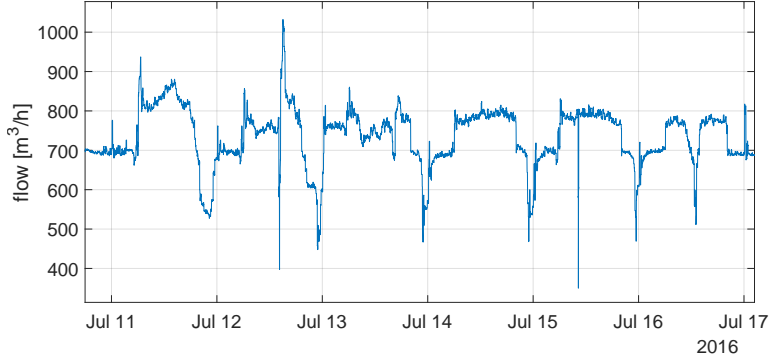


Figure 5: Trend of $w_{hot}(t)$

1. $T_i(t)$ and $T_o(t)$, i.e. the delivery and return manifold water temperatures.
2. Temperature measures along the three collectors to/from the users (see Figure 2). We computed their average on the return collectors, weighted by their flowrates, and named it $T_{hot}(t)$.
3. Temperature measures across the eight end-users, both on the inlet and outlet sides, named $T_{in}^j(t)$ and $T_{out}^j(t)$ respectively, $j = 1, \dots, 8$. We indicate their weighted average values with $\bar{T}_{in}(t)$ and $\bar{T}_{out}(t)$, more precisely:

$$\bar{T}_{in}(t) = \frac{\sum_{j=1}^8 T_{in}^j(t)w_u^j(t)}{w_{hot}(t)}, \quad \bar{T}_{out}(t) = \frac{\sum_{j=1}^8 T_{out}^j(t)w_u^j(t)}{w_{hot}(t)} \quad (4)$$

At first we checked consistency of the available data, so we compared $T_o(t)$ with $T_{hot}(t)$ and $\bar{T}_{out}(t)$. The comparison is shown in Figure 6. First we can notice that $\bar{T}_{out}(t)$ is significantly biased, secondly in some periods also $T_{hot}(t)$ is higher than $T_o(t)$. These discrepancies can not be due to the effects of the solar radiation along the pipes, or to the thermal exchange with the environment, since these phenomena would produce the opposite effect. Therefore, the most likely reason is the bypass valve, that directly circulates cold water from the delivery manifold to the return manifold, thus decreasing the temperature in the latter. This is confirmed by the fact that this bias occurs only when many machines are active, as visible again in Figure 6 where the number of active machines $n_{on}(t) = \sum_{i=1}^4 s_i(t) + s_{abs}(t)$ is represented in dashed line. Unfortunately no measure of the by-pass flowrate $w_{bp}(t)$ is available; this additional information is fundamental to define the overall model of the system, so we had to estimate it as described in Section 4.2.4.

On the delivery side, we first compared $T_i(t)$ with the three temperature measures on the delivery collectors, that exhibit the same pattern, see Figure

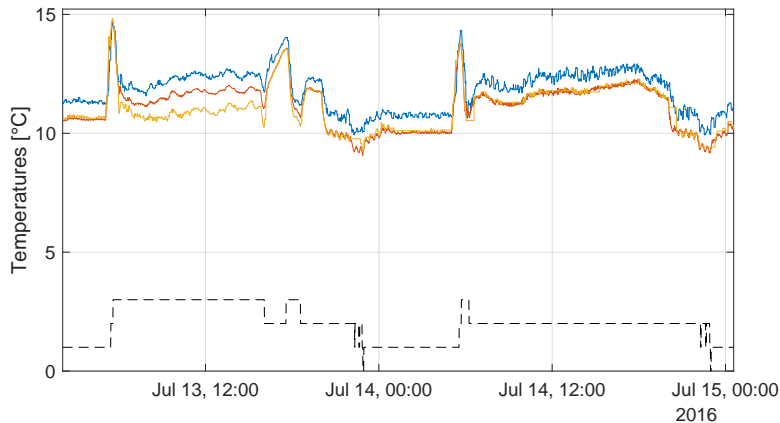


Figure 6: Comparison of the return temperature measures. Blue line: $\bar{T}_{out}(t)$; red line: $T_{hot}(t)$, yellow line: return manifold $T_o(t)$. Dashed line: $n_{on}(t)$

7, though a small bias (0.3 °C) is sometimes present in one of the collectors, possibly due to the drift of one sensor. Indeed, by comparing $T_i(t)$ with the inlet measures on the end-users $T_{in}^j(t)$, a significant difference appears again, as well as on the return side, as reported for completeness in Figure 8.

4. Model Identification

4.1. Adopted modelling approach

The model for the overall system has been obtained by connecting the models of the following subsystems: the chillers with their evaporative towers, the absorber, the end-users, and the piping system. These models are either static or dynamic, and have been estimated from data according to the following procedure, unless they directly follow from physical relations:

- In the identification phase, linear model structures, including AutoRegressive-Exogenous (ARX), AutoRegressive-Moving-Average Exogenous (ARMAX), Output-Error (OE), see [17], have been first considered. More complex models, e.g. polynomial models and Neural Networks (NN), have been employed only when the first proved to be inadequate.
- According to a well-established procedure, see [17], the identification phase has been performed on a subset of the data (*identification set*), while the model performances have been cross-validated on another subset (*validation set*).
- The regressors to be included in the models have been chosen based on two principles: first we have chosen the variables that are known to mostly

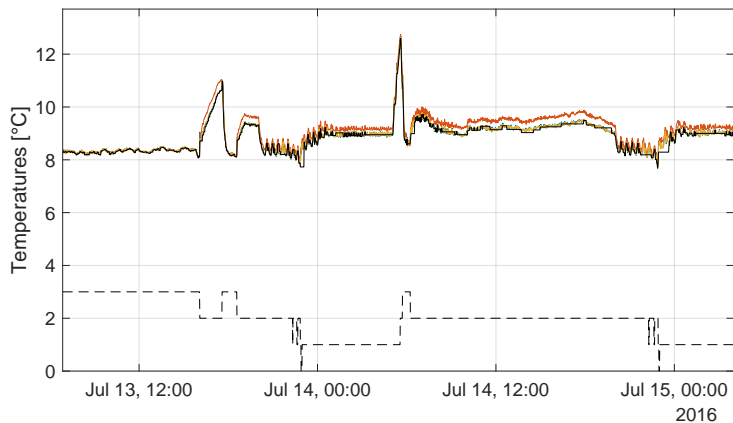


Figure 7: Comparison of the delivery temperature measures. Black line: delivery manifold T_i measure, bright lines: measures on delivery collectors. Dashed line: $n_{on}(t)$

influence the output from physical considerations, then we have selected the most influencing regressors with a feature selection technique based on the LASSO algorithm [28]. In this approach, it is assumed that the output of the model y depends linearly on the vector of parameters θ to be estimated, through the relation $y(t) = \theta^T \varphi(t)$, where t is the discrete time variable, φ is the vector of regressors and T is the vector transpose operation. Note that $\varphi(t)$ can be a nonlinear function of measured quantities. First, a Least Square problem including a large number of candidate regressors is solved, and its mean prediction squared error ϵ^2 is computed. Then, a first estimate of θ is obtained by solving the modified least squares problem

$$\begin{aligned} \min_{\theta} \quad & \|\theta\|_1 \\ \text{s.t.} \quad & \frac{1}{N} \sum_{i=1}^N (y(t) - \theta^T \varphi(t))^2 < \gamma \epsilon^2 \end{aligned} \quad (5)$$

where N is the total number of available observations and $\gamma > 1$ is a conservative factor. Finally, the elements of the estimated vector θ with smaller absolute value (e.g. those below $\frac{1}{100}$ of the maximum), which contribute less to compute the output, are removed from the model together with the corresponding regressors. The last step of the algorithm consists in retraining the model with the regressors selected in the first phase.

4.2. Model identification results

The models of the different subsystems are described next.

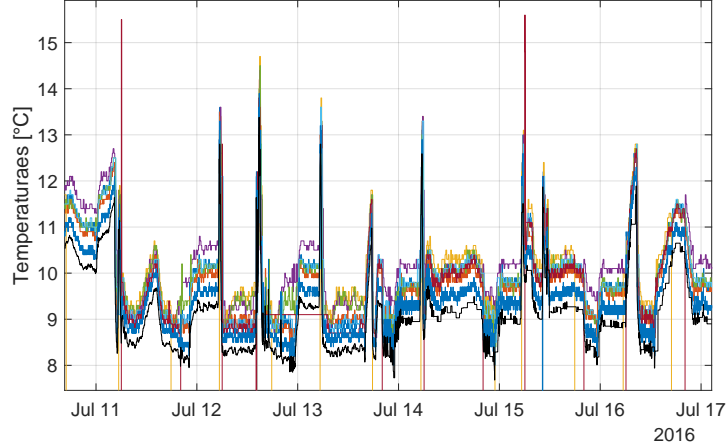


Figure 8: Comparison of the delivery temperature measures. Black line: delivery manifold T_i measure, bright lines: measures on end-users.

4.2.1. Chillers and evaporative towers

Chiller cooled water temperature

The temperature of the cooled water $T_r^i(t)$, see Figure 4, is one of the most meaningful variables of the chiller. As anticipated, each time the chiller is activated, it settles to the desired setpoint $T_r^{sp} = 8$ °C. Typical transients are reported in Figure 9, which shows that AutoRegressive models (AR) are suitable to describe this dynamics. More specifically, the error variable is defined as

$$e(t) = T_r^{sp} - T_r^i(t), \quad i = 1, 2, 3, 4 \quad (6)$$

and estimated the parameters of the second-order AR model

$$e(t) = a_1 e(t-1) + a_2 e(t-2) \quad (7)$$

The choice of a second-order model is motivated by the two physical phenomena of the system: the cooling of the heat exchanger inside the chiller, with a faster time constant, and the thermal exchange with the cooled water, with a slower time constant. The model has been identified with the data collected on chiller 4 and validated against other chillers, always leading to satisfactory results, see again Figure 9. In chiller *off* conditions, $T_r^i(t)$ is meaningless for the thermal balance, moreover its measurements are affected by drifts, possibly due to the external temperature and the solar radiation warming.

Chiller condenser output temperature

The condenser output temperature $T_c^i(t)$, $i = 1, \dots, 4$ has a significant influence upon the chiller's efficiency, see [29] and [11]. As shown in Figure 4, $T_c^i(t)$

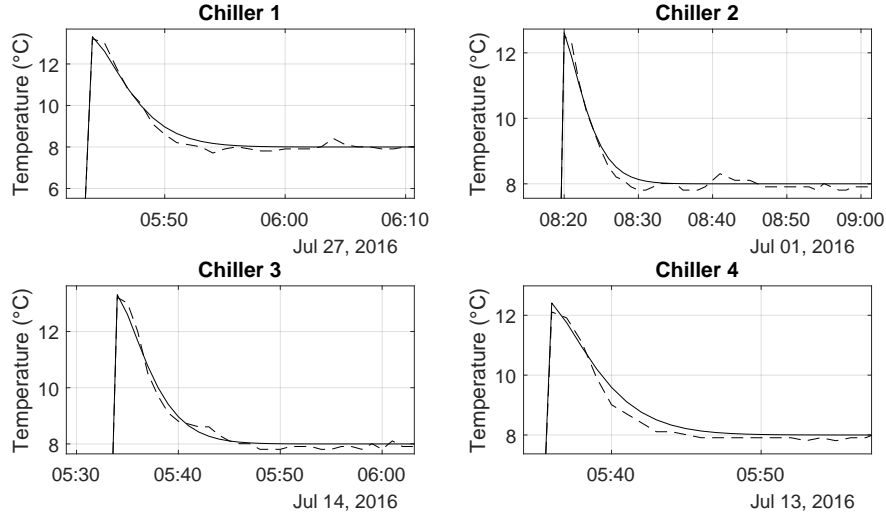


Figure 9: Chiller cooled water temperature. Comparison between real data and model response for $T_r^i(t)$, $i = 1, 2, 3, 4$ with validation data. Solid line: model response, dashed line: real data

depends on the water temperature from the return manifold $T_{in}^i(t)$, on the environmental conditions expressed by the ambient temperature and humidity, $T_{ext}(t)$ and $H_{ext}(t)$, respectively, on the chiller cooled water temperature $T_r^i(t)$ (the output of the model previously described), and on the command $v^i(t)$ to the tower fans. These variables have been considered as inputs of a second order Output Error (OE) model, which represents a satisfactory compromise between accuracy and simplicity. The delays between inputs and output have been selected to be zero for all the inputs, save for the one related to $v^i(t)$, which has been set equal to one, since this signal acts on the tower and is physically detached from the chiller. Figure 10 shows the comparison between real data and model responses for $T_c^i(t)$, the latter identified on Chiller 4. The performance is satisfactory despite the many uncertainties, for instance the fact that the relative humidity measure is corrupted by a non negligible measurement noise. Again, the model is valid for the *on* condition of the chillers, while there is no utility in modeling $T_c^i(t)$ during the *off* phases.

Chiller Regulator identification

The identification of the regulator computing the command to the fans $v^i(t)$ is required to simulate the model of $T_c^i(t)$. The following assumptions, to be validated *a-posteriori*, have been made: (i) the controller is a Proportional-Integral (PI) one, (ii) the controlled variable is $T_c^i(t)$, as confirmed by the plant

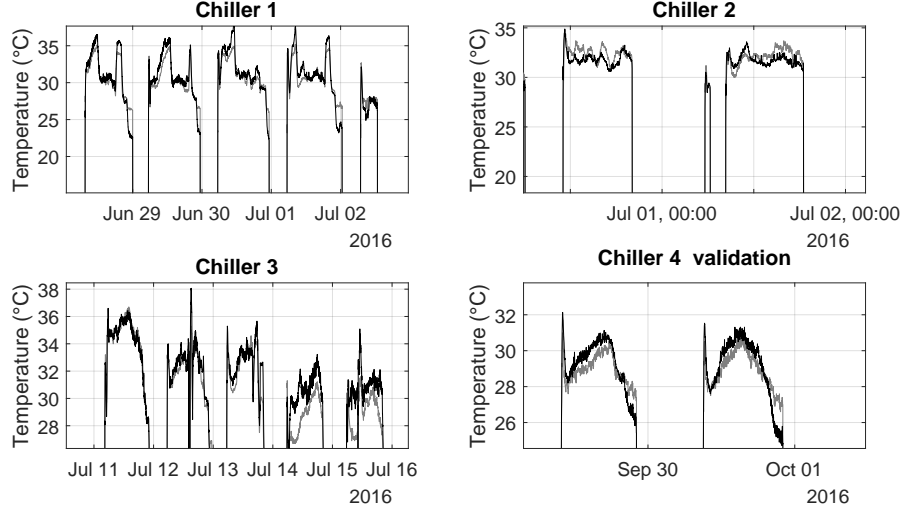


Figure 10: Chiller condenser output temperature. Comparison between real data and model response for $T_c^i(t)$, $i = 1, 2, 3, 4$. Dark line: model response, light line: real data

operators, (iii) the setpoint is 24 °C, as often specified in the guidelines of chiller manufacturers. The identification has been performed according to a *direct approach*, i.e. with the input-output data of the controller, neglecting the feedback effect, see [10]. The proportional and integral gains $K_p = -25$ and $K_i = -1.5 \times 10^{-5}$ have been obtained. In addition, it has been verified that the PI has been implemented without an *anti wind-up* scheme, that would be recommendable since the control input is often saturated, and without the reset of the initial condition at every switch of the chiller. The performances provided by the identified controller confirm the previous assumptions and can be considered satisfactory, as shown in Figure 11.

Chiller Power consumption

A detailed model of the chillers power consumption $P^i(t)$, $i = 1, \dots, 4$ is needed to properly state a control problem aimed at optimizing the managing costs. Starting from physical considerations, we first selected the following variables, assumed to be the most influencing ones: $T_{in}^i(t)$, $T_r^i(t)$ (obtained with the identified model specified in Section 4.2.1), the external conditions $T_{ext}(t)$ and $H_{ext}(t)$, the control variable $v^i(t)$, and $T_c^i(t)$, that is known from literature to influence the absorbed power. We *a-priori* considered as regressors all polynomials of first and second order, including cross-products of the selected variables. This choice is motivated by the physical insight that power is proportional to the square of some of the involved variables, in particular temperatures. Static

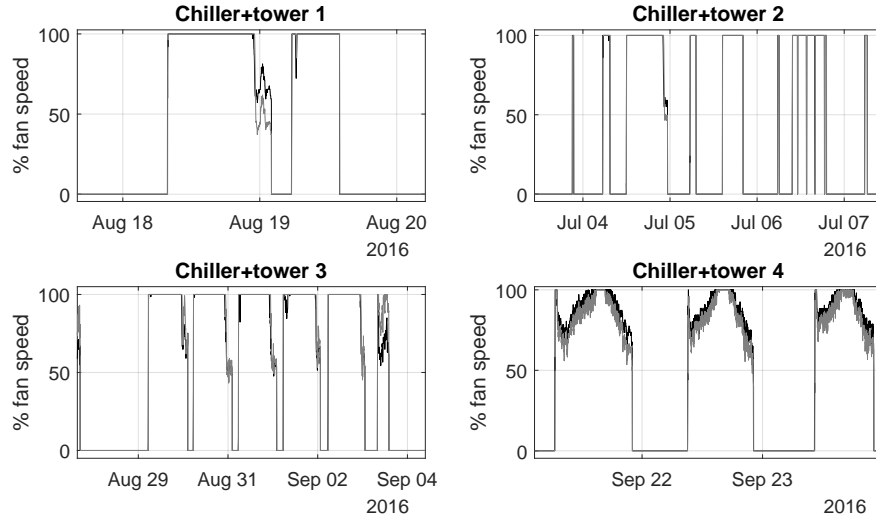


Figure 11: Chiller regulator. Comparison between real data and model response for $v^i(t)$, $i = 1, 2, 3, 4$. Dark line: identified regulator response, light line: real data

models have been estimated, since from the physics it is reasonable to assume that possible delays between the model inputs and the power itself are negligible with respect to the adopted sampling time $T_s = 60$ s. The identification procedure led to a model that is able to properly describe the power consumption (see Figure 12), although sometimes less performing when applied to the data of chiller 1. This could be due to the different wear of the chiller and/or to the measurement noise related to the temperatures sensors.

4.2.2. Users

As anticipated, the users are distributed over the five buildings, and very little information is available on their dynamical behavior. A modeling approach based on physical equations would be infeasible in this case, given the complexity of the process, the lack of information, and the sparse layout of the end-users. The main quantity to be described, in order to properly simulate the system and to reproduce the water heating dynamics, is the thermal power $Q_u(t)$ requested by all the users. With reference to the j -th end-user, the thermal power $Q_u^j(t)$ can be computed as

$$Q_u^j(t) = \rho_w c_w w_u^j(t) (T_{out}^j(t) - T_{in}^j(t)) \quad (8)$$

where c_w is the specific heat of the water and $w_u^j(t)$ is the water flowing through the user's cooling circuit. This computation has been made with the flowrate measurements associated with the end-users, and not with the ones

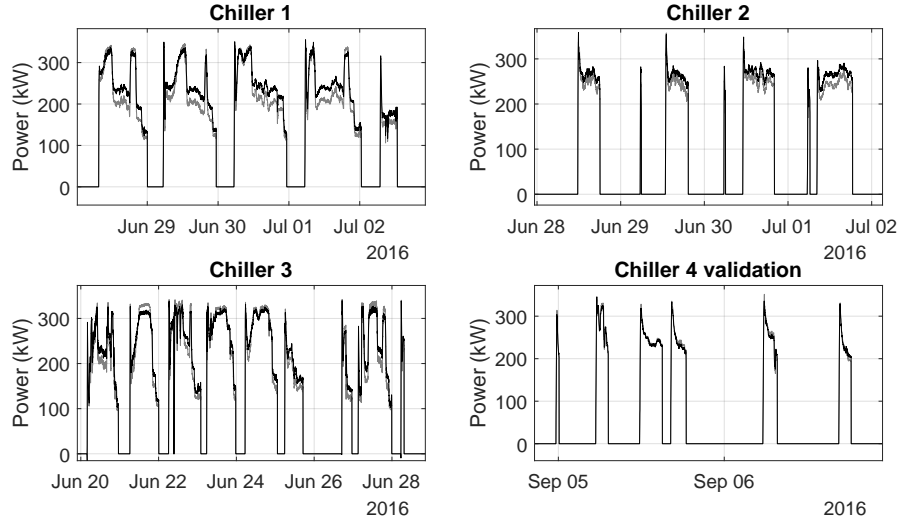


Figure 12: Chiller power consumption. Comparison between real data and model response for $P^i(t)$, $i = 1, 2, 3, 4$. Dark line: model response, light line: measured data

related to the delivery and return collectors, to mitigate as much as possible the effect of transport delays. Eventually the total thermal power is computed by summing all the end-users contributions:

$$Q_u(t) = \sum_{j=1}^8 Q_u^j(t) \quad (9)$$

In principle, the required thermal power depends on the environmental conditions (represented by $H_{ext}(t)$ and $T_{ext}(t)$), on the day of the week, and on the hour of the day. For this reason, we have estimated two different models: one for the working days (Monday-Friday), and one for the weekends (Saturday and Sunday). As additional inputs, besides $H_{ext}(t)$ and $T_{ext}(t)$, the minute of the day has been considered. In the working days this input goes from 1 (midnight) to 1440 (23:59), while for the weekends it goes from 1 to 2880, so as to distinguish between Saturdays and Sundays. The adopted model structure is a static neural network with one hidden layer and twenty neurons.

The model outputs are compared to the real data in Figures 13 (for weekdays), and 14 (for weekends). It is apparent that the network is capable to reproduce well the computed quantity $Q_u(t)$, and especially the low-frequency components of the signal. The higher frequencies are due to switching and short-term regulations of the cooling machines at the users' side, that are totally unknown and unpredictable, and have to be accounted for as a disturbance

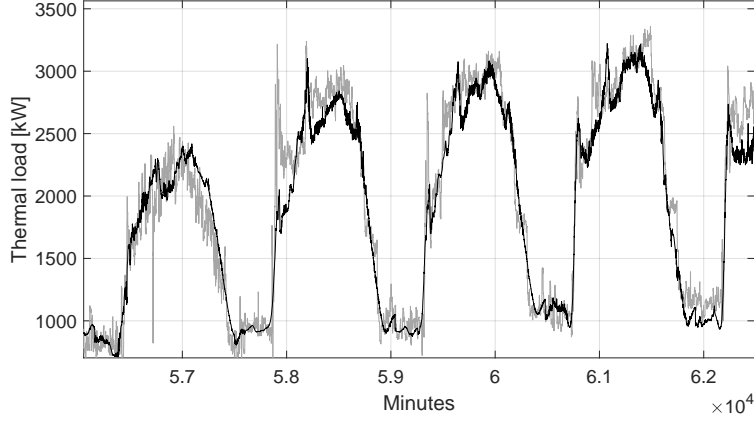


Figure 13: Thermal load of the users during working days. Light line: real computed value $Q_u(t)$. Black line: predicted value

against which the cooling station has to react. Note that in Figure 14 the samples corresponding to different weekends are merged, so that the timescale is not continuous.

4.2.3. Pipes

The pipes are among the most uncertain parts of the system, since no parameters are available on their length and section, and they can not be neglected both in terms of heat exchanged with the environment and of transport delay. Given the lack of information, and based on very rough estimates, the following simplifying assumptions have been introduced: (i) the five tubes out of the chillers and the absorber have radius $R = 0.1$ m and converge to the delivery manifold, whose cross-section is equal to the sum of sections of the inlet pipes, (ii) the average length from the cooling station to the end-users is $L = 80$ m. Considering an average value for $w_t(t)$ equal to $\tilde{w}_t = 750\text{m}^3/\text{h}$ (see Figure 5), the average speed \tilde{v} is computed as:

$$\tilde{v} = \left(\frac{\tilde{w}_t}{3600} \right) / (5\pi R^2) \quad (10)$$

and the transport delay is estimated as:

$$\Delta t_d = \frac{L}{\tilde{v}} \sim 60.31\text{s} \quad (11)$$

which is close to the adopted sampling time $T_s = 1$ min. Thus, the unitary delay is added both on the forward and on the return line (see Figure 3)

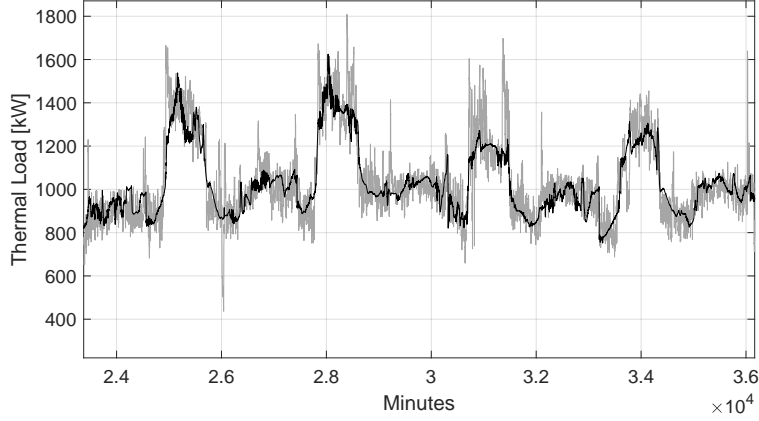


Figure 14: Thermal load of the users during weekends. Data merged from non-contiguous days. Light line: real computed value $Q_u(t)$. Black line: predicted value

Assuming the average overall heat transfer coefficient $k = 50 \frac{W}{m^2K}$, taken from [15], the thermal power exchanged with the external environment can be computed as:

$$Q_{pipes}(t) = \frac{k}{1000} 2\pi R_{eq} 2L (T_{ext}(t) - T_i(t)) \quad (12)$$

where $R_{eq} = \sqrt{\frac{5\pi R^2}{\pi}}$ is the radius of the delivery manifold tube, and the length L is considered twice to account for the delivery and return paths. The bias present on the sensors at the inlet side of end-users, see Section 3, does not allow one to validate these equations, that are hence tested with the closed-loop temperatures of the delivery and return manifolds in Section 5.

4.2.4. Estimate of the bypass flowrate and hydraulic balance of the loops

For the estimation of the bypass flowrate $w_{bp}(t)$ and of the flowrate $w_{off}(t)$ through the chillers in *off* mode, reference is made to the scheme of Figure 3. The developments are mainly based on static thermal balances. To this end, preliminarily define $w_{on}(t)$ as the sum of flowrates through the active machines:

$$w_{on}(t) = \sum_{i=1}^4 s_i(t) w_{ch} + s_{abs}(t) w_{abs} \quad (13)$$

From the mass balance equation of the (primary and secondary) loops, see Figure 3, we can write:

$$w_t(t) = w_{on}(t) + w_{off}(t) = w_{hot}(t) + w_{bp}(t) \quad (14)$$

The flowrates $w_{off}(t)$ and $w_{bp}(t)$ account for the mismatch between the water required by the utilities $w_{hot}(t)$, pumped by a dedicated and independent set of pumps, and $w_{on}(t)$, that instead is ruled by the control logic of the plant.

The estimator of $w_{off}(t)$ and $w_{bp}(t)$ distinguishes two cases, i.e.:

- If $w_{on}(t) < w_{hot}(t)$, then $w_{bp}(t) = 0$ and $w_{off}(t) = w_{hot}(t) - w_{on}(t)$.

In this condition, the users require a significant amount of water, and the active machines pump less flow rate, so that $w_{off}(t) > 0$, while $w_{bp}(t)$ is assumed to be zero.

- If $w_{on}(t) > w_{hot}(t)$, then $w_{bp}(t) = -(w_{hot}(t) - w_{on}(t))$ and $w_{off}(t) = 0$.

In this case, the active machines pump more water than that required by users, thus imposing the total flow of the primary loop and forcing a non null value of $w_{bp}(t)$. The flowrate $w_{off}(t)$, on the other hand, is null, since active machines provide enough flow to feed the users.

In both cases, we can write the thermal balance equation related to the users as

$$T_{hot}(t) = T_i(t) + \frac{Q_u(t) + Q_{pipes}(t)}{\rho_w c_w w_{hot}(t)} \quad (15)$$

Given that no measures of $w_{bp}(t)$ and $w_{off}(t)$ are available, their estimates can be validated only through the temperature predictions obtained from the simulation of the whole plant, as reported in the next section.

5. Closed-loop validation

The models of the subsystems have been linked together according to the layout of the plant, see Figure 3, and a simulator of the overall system has been developed in the Matlab/Simulink environment.

The temperature $T_i(t)$ in the delivery manifold has been computed as follows. First, the auxiliary variable $T_r^{on}(t)$ has been computed as the average, weighted by the flow rates, of the temperatures due to the active machines:

$$T_r^{on}(t) = \frac{\sum_{i=1}^4 s_i(t) T_r^i(t) w_{ch} + s_{abs}(t) T_r^{abs}(t) w_{abs}}{w_{on}(t)} \quad (16)$$

Then, $T_i(t)$ has been obtained as the weighted contribution of the active machines and of the water passing through the chillers in *off* mode, that flows at temperature $T_o(t)$:

$$T_i(t) = \frac{w_{on}(t) T_r^{on}(t) + w_{off}(t) T_o(t)}{w_t(t)} \quad (17)$$

In a similar way, it is possible to compute the temperature $T_o(t)$ in the return manifold, given by

$$T_o(t) = \frac{w_{hot}(t)T_{hot}(t) + w_{bp}(t)T_i(t)}{w_t(t)} \quad (18)$$

The transients of $T_i(t)$ and $T_o(t)$, computed with the simulator, are compared to the corresponding measured values in Figures 15 and 16, which show the effectiveness of the adopted modeling approach for the overall system. Performances are less satisfactory during the weekend (16-18 July) since the chillers are nearly always off, as shown in Figure 17, so that the plant is more sensitive to unmodelled disturbances raising from the users and the absorber, that are the only active components. The root mean square error is 0.35 °C for the delivery temperature T_i , and 0.5 °C for the return temperature T_o . These are acceptable values given the present uncertainty.

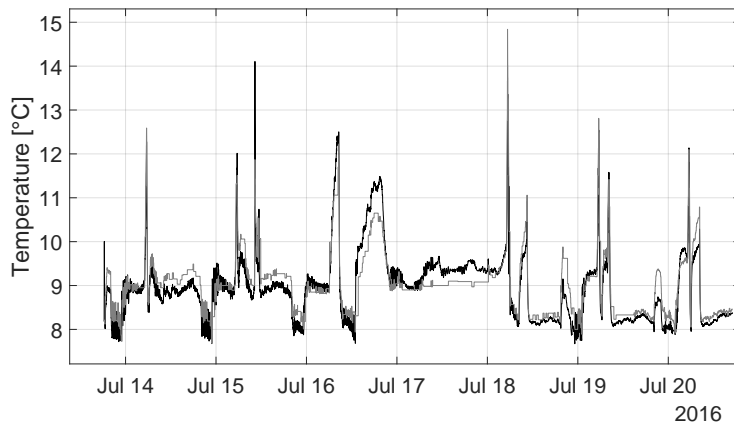


Figure 15: Closed-loop validation. Delivery manifold temperature T_i . Black line: simulated value. Grey line: real value

6. Control design and performance evaluation

The plant is controlled using a relay-based logic, which rules when to switch chillers *on* and *off*. The controller includes also a minimal idle time to be observed, denoted by D_t , after the switching of a chiller, in order to wait for its effect to completely influence the temperatures and avoid too frequent commutations. The conditions implemented in the control logic and governing the switches are based on $T_i(t)$ and $T_o(t)$, and are reported in the following tables 1 and 2, related to the *on* and *off* switching cases, respectively.

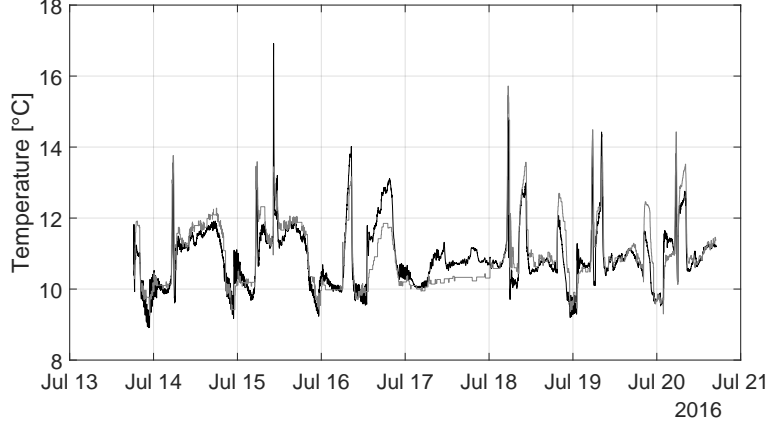


Figure 16: Closed-loop validation. Return manifold temperature T_o . Black line: simulated value. Grey line: real value

ON Switching		
$T_i > \underline{\tau}_{on,1}$	$T_o > \bar{\tau}_{on,1}$	Chiller 1
$T_i > \underline{\tau}_{on,2}$	$T_o > \bar{\tau}_{on,2}$	Chiller 2
$T_i > \underline{\tau}_{on,3}$	$T_o > \bar{\tau}_{on,3}$	Chiller 3
$T_i > \underline{\tau}_{on,4}$	$T_o > \bar{\tau}_{on,4}$	Chiller 4

Table 1: Control logic: on switching temperature conditions

$\underline{\tau}_{on,k} < \underline{\tau}_{on,k+1}$ and $\bar{\tau}_{on,k} < \bar{\tau}_{on,k+1}$, $k = 1, 2, 3$ are tuning parameters, whose values are not reported here for confidentiality reasons. The logic governing the switch *off* of the chillers is dual,

where again $\underline{\tau}_{off,k} < \underline{\tau}_{off,k+1}$ and $\bar{\tau}_{off,k} < \bar{\tau}_{off,k+1}$, $k = 1, 2, 3$.

Every condition on the temperature must be fulfilled for a period longer than $\Delta T_{temp} = 300$ s before producing a switch, and it is possible to switch only one chiller at a time. The subsequent commutation can take place only after a fixed idle time D_t , set equal to 10 minutes, provided that the associated conditions hold. This is designed to avoid activating chillers only because temperatures are raising suddenly, for example in the early morning when the load increases, but only one chiller is enough to control the system.

Optimization of the control logic

The settings of the parameters of the control logic are manually driven and based on empirical rules. As an alternative, due to the availability of the identified model described in the previous sections, in this paper it is proposed to tune

OFF switching		
$T_i < \underline{\tau}_{off,1}$	$T_o < \bar{\tau}_{off,1}$	Chiller 1
$T_i < \underline{\tau}_{off,2}$	$T_o < \bar{\tau}_{off,2}$	Chiller 2
$T_i < \underline{\tau}_{off,3}$	$T_o < \bar{\tau}_{off,3}$	Chiller 3
$T_i < \underline{\tau}_{off,4}$	$T_o < \bar{\tau}_{off,4}$	Chiller 4

Table 2: Control logic: off switching temperature conditions

these parameters by solving an optimal control problem. More specifically, we have introduced three optimization variables ΔT_{on} , ΔT_{off} , ΔD_t and modified the temperatures thresholds and the idle time as follows:

$$\begin{aligned}
\tilde{\tau}_{on,k} &= \tau_{on,k} + \Delta T_{on} \\
\tilde{\tau}_{on,k} &= \bar{\tau}_{on,k} + \Delta T_{on} \\
\tilde{\tau}_{off,k} &= \tau_{off,k} + \Delta T_{off}, \quad k = 1, 2, 3, 4 \\
\tilde{\tau}_{off,k} &= \bar{\tau}_{off,k} + \Delta T_{off} \\
\tilde{D}_t &= D_t + \Delta D_t
\end{aligned} \tag{19}$$

The objective function takes into account both the performances of the plant, measured in terms of discomfort, and its running cost. As for the first, since the plant is devoted to serving utilities and satisfying their load demand, we have weighted the mismatch between the cooling power and the load demand in absolute value. Specifically, we have defined the global cooling power provided by the cooling machines as:

$$Q_{refr}(t) = c_w \rho_w w_t(t) (T_i(t) - T_o(t)) \tag{20}$$

As for the running cost, it is directly proportional to the absorbed power, that has been modelled as described in Section 4.2.1. Therefore, this term must also be included in the cost function.

The optimization problem takes the following form:

$$\begin{aligned}
&\min_{\Delta T_{on}, \Delta T_{off}, \Delta D_t} \int_{t_0}^{t_f} \sum_{i=1}^4 P_{ch}^i(t) + \alpha |Q_u(t) + Q_{pipes}(t) + Q_{refr}(t)| dt \\
&\text{subject to } \underline{\Delta T}_{on} \leq \Delta T_{on} \leq \bar{\Delta T}_{on} \\
&\quad \underline{\Delta T}_{off} \leq \Delta T_{off} \leq \bar{\Delta T}_{off} \\
&\quad \underline{\Delta D}_t \leq \Delta D_t \leq \bar{\Delta D}_t
\end{aligned} \tag{21}$$

where $\underline{\Delta T}_{on}$, $\bar{\Delta T}_{on}$, $\underline{\Delta T}_{off}$, $\bar{\Delta T}_{off}$ and $\underline{\Delta D}_t$, $\bar{\Delta D}_t$ are lower and upper bounds on the optimization variables.

The reference week from July 14th to 20th has been taken as the interval of

Baseline	
$\int_{t_0}^{t_f} Q_u(t) + Q_{pipes}(t) + Q_{refr}(t) dt$	$\int_{t_0}^{t_f} \sum_{i=1}^4 P_{ch}^i(t) dt$
$1.33 \times 10^4 kWh$	$2.83 \times 10^4 kWh$

Optimized logic ($\alpha = 1$)	
$\int_{t_0}^{t_f} Q_u(t) + Q_{pipes}(t) + Q_{refr}(t) dt$	$\int_{t_0}^{t_f} \sum_{i=1}^4 P_{ch}^i(t) dt$
$1.36 \times 10^4 kWh$	$1.92 \times 10^4 kWh$

Table 3: Comparison between the current and the optimized control logic on the plant

optimization $[t_0, t_f]$, which is the same period reported for the validation of the models in Figures 15 and 16.

The nonlinear optimization problem has been solved with the *fmincon* routine available in Matlab. The computed optimal solution is $\Delta D_t^o = 0\text{min}$, $\Delta T_{on}^o = 2^\circ\text{C}$, $\Delta T_{off}^o = 1^\circ\text{C}$. From a physical standpoint, the optimized parameters imply that the idle time is not changed, but the thresholds are raised both for the *on* and *off* switching. In practice, the chillers switch *on* when the temperature is higher than before. The control logic has been implemented in the plant simulator, and experiments have been performed with both the original and the optimized control. Some of the results achieved are reported in Figure 17, which shows that the optimized logic drives the plant to a more regular control pattern, avoiding the switching of the chillers when not necessary, and exploiting completely one chiller in place of having two machines not working at full capability. Indeed, the new thresholds are such that the switching *off* of one chiller for a short period of time, followed by its new activation, is avoided, see again Figure 17. A comparison between the current and the optimized logic performances acting on the plant is reported in Table 3.

The table shows that, at the price of an increase of about 2.5% of the discomfort term $|Q_u(t) + Q_{pipes}(t) + Q_{refr}(t)|$, the power consumption is reduced of about 30%, thus motivating the use of the optimized parameters.

7. Conclusions

A structured black-box approach for modelling a cooling station serving a large business center has been presented. It relies on a very large data-set employed to derive models of the subsystems composing the plant, eventually connected together according to the actual plant schematic. Modelling performance proved to be satisfactory despite the critical uncertainties present in the problem. Based on the obtained model, the parameters of the currently adopted control logic have been optimized, leading to promising results in terms of en-

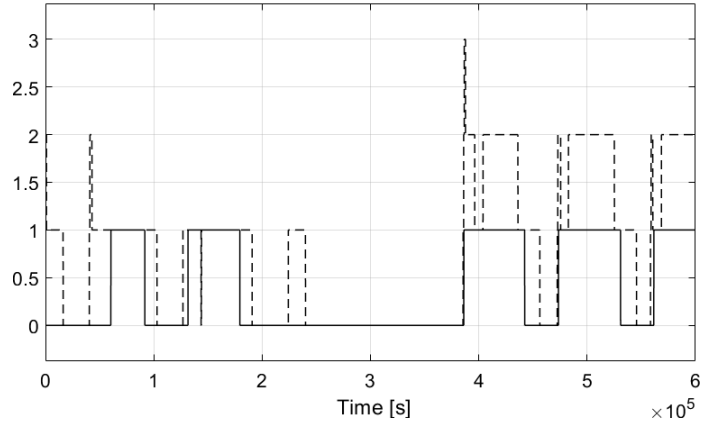


Figure 17: Comparison between the number of active chillers with current and optimized control logic. Solid line: optimized, dashed line: current logic

ergy savings. The proposed approach allows one to quickly model similar plants by suitably composing their constituting subsystems, and the control approach does not require any hardware nor software modification, leading to a simple but effective strategy.

Future work will concern both the test on the real plant and the development of a hybrid Model Predictive Controller, possibly with a more intense use of black box estimation techniques, for instance neural networks, to reduce the modelling efforts.

References

- [1] Abdul Afram, Alan S Fung, Farrokh Janabi-Sharifi, and Kaamran Raahemifar. Development and performance comparison of low-order black-box models for a residential hvac system. *Journal of Building Engineering*, 15:137–155, 2018.
- [2] A Allouhi, Y El Fouih, T Kousksou, A Jamil, Y Zeraoui, and Y Mourad. Energy consumption and efficiency in buildings: current status and future trends. *Journal of Cleaner production*, 109:118–130, 2015.
- [3] Fatima Amara, Kodjo Agbossou, Alben Cardenas, Yves Dubé, and Sousso Kelouwani. Comparison and simulation of building thermal models for effective energy management. *Smart Grid and renewable energy*, 6(04):95, 2015.
- [4] Sina Faizollahzadeh Ardabili, Asghar Mahmoudi, and Tarahom Mesri Gundoshmian. Modeling and simulation controlling system of hvac using fuzzy

- and predictive (radial basis function, rbf) controllers. *Journal of Building Engineering*, 6:301–308, 2016.
- [5] Alessandro Beghi, Luca Cecchinato, Mirco Rampazzo, and Francesco Simmini. Energy efficient control of hvac systems with ice cold thermal energy storage. *Journal of process control*, 24(6):773–781, 2014.
- [6] Yunus A Cengel and Michael A Boles. Thermodynamics: an engineering approach. *Sea*, 1000:8862, 2002.
- [7] Jiri Cigler, Dimitrios Gyalistras, Jan Široky, V Tiet, and Lukaš Ferkl. Beyond theory: the challenge of implementing model predictive control in buildings. In *Proceedings of 11th Rehva world congress, Clima*, volume 250, 2013.
- [8] LEED Steering Committee et al. Foundations of the leadership in energy and environmental design environmental rating system: A tool for market transformation. *LEED Policy Manual*. US Green Building Council, 2003.
- [9] Ján Drgoňa, Damien Picard, Michal Kvasnica, and Lieve Helsen. Approximate model predictive building control via machine learning. *Applied Energy*, 218:199–216, 2018.
- [10] Urban Forsell and Lennart Ljung. *Closed-loop identification revisited*. Linköping University Electronic Press, 1997.
- [11] James W Furlong, Frank T Morrison, et al. Optimization of water-cooled chiller-cooling tower combinations. *CTI journal*, 26(2):14, 2005.
- [12] Gohar Gholamibozanjani, Joan Tarragona, Alvaro de Gracia, Cèsar Fernández, Luisa F Cabeza, and Mohammed M Farid. Model predictive control strategy applied to different types of building for space heating. *Applied Energy*, 231:959–971, 2018.
- [13] Phillip Haves. Model predictive control of hvac systems: Implementation and testing at the university of california, merced. 2010.
- [14] Ron Judkoff and Joel Neymark. International energy agency building energy simulation test (bestest) and diagnostic method. Technical report, National Renewable Energy Lab., Golden, CO (US), 1995.
- [15] Donald Quentin Kern. *Process heat transfer*. Tata McGraw-Hill Education, 1950.
- [16] Jens Laustsen. Energy efficiency requirements in building codes, energy efficiency policies for new buildings. *International Energy Agency (IEA)*, 2(8):477–488, 2008.
- [17] Lennart Ljung. System identification. In *Signal analysis and prediction*, pages 163–173. Springer, 1998.

- [18] Yudong Ma, Anthony Kelman, Allan Daly, and Francesco Borrelli. Predictive control for energy efficient buildings with thermal storage: Modeling, stimulation, and experiments. *IEEE Control Systems*, 32(1):44–64, 2012.
- [19] Yudong Ma, Jadranko Matuško, and Francesco Borrelli. Stochastic model predictive control for building hvac systems: Complexity and conservatism. *IEEE Transactions on Control Systems Technology*, 23(1):101–116, 2015.
- [20] Houcem Eddine Mechri, Alfonso Capozzoli, and Vincenzo Corrado. Use of the anova approach for sensitive building energy design. *Applied Energy*, 87(10):3073–3083, 2010.
- [21] F.W. Payne and J.J. McGowan. *Energy management and control systems handbook*. Fairmont Press, 1988.
- [22] Ethan Png, Seshadhri Srinivasan, Korkut Bekiroglu, Jiang Chaoyang, Rong Su, and Kameshwar Poolla. An internet of things upgrade for smart and scalable heating, ventilation and air-conditioning control in commercial buildings. *Applied Energy*, 239:408–424, 2019.
- [23] Roozbeh Sangi, Alexander Kümpel, and Dirk Müller. Real-life implementation of a linear model predictive control in a building energy system. *Journal of Building Engineering*, 22:451–463, 2019.
- [24] Harish Satyavada and Simone Baldi. An integrated control-oriented modelling for hvac performance benchmarking. *Journal of Building Engineering*, 6:262–273, 2016.
- [25] Francesco Smarra, Achin Jain, Tullio de Rubeis, Dario Ambrosini, Alessandro D’Innocenzo, and Rahul Mangharam. Data-driven model predictive control using random forests for building energy optimization and climate control. *Applied Energy*, 2018.
- [26] Jian Sun and Agami Reddy. Optimal control of building hvac&r systems using complete simulation-based sequential quadratic programming (csb-sqp). *Building and environment*, 40(5):657–669, 2005.
- [27] E. Terzi, L. Fagiano, M. Farina, and R. Scattolini. Identification of the cooling system of a large business center. *IFAC-PapersOnLine*, 51(15):174 – 179, 2018. 18th IFAC Symposium on System Identification SYSID 2018.
- [28] Robert Tibshirani. Regression shrinkage and selection via the lasso. *Journal of the Royal Statistical Society. Series B (Methodological)*, pages 267–288, 1996.
- [29] Xiupeng Wei, Guanglin Xu, and Andrew Kusiak. Modeling and optimization of a chiller plant. *Energy*, 73:898–907, 2014.
- [30] Zhou Xuan, Zi Xuehui, Liang Liequan, Fan Zubing, Yan Junwei, and Pan Dongmei. Forecasting performance comparison of two hybrid machine learning models for cooling load of a large-scale commercial building. *Journal of Building Engineering*, 21:64–73, 2019.